Nasal Epithelial Permeation of Thymotrinan (TP3) Versus Thymocartin (TP4): Competitive Metabolism and Self-Enhancement

M. Christiane Schmidt,[1,3] Werner Rubas,[2] and Hans P. Merkle[1,4]

Received September 22, 1999; accepted November 12, 1999

Purpose. To investigate concentration dependent permeabilities and metabolism kinetics of thymotrinan (TP3) versus thymocartin (TP4) in nasal epithelium in vitro.

Methods. Excised bovine nasal mucosa was used as an in vitro model. Permeabilities were studied in a diffusion chamber, metabolism kinetics in a reflection kinetics set-up. Studies were performed at various TP3 and TP4 concentrations. The ^{3}H-mannitol flux was measured to monitor junctional permeability. Potential Ca^{2+}-complexation was investigated using a Ca^{2+}-selective electrode.

Results. Permeability of TP3 was negligible at 0.1 and 0.2 mM and increased drastically above 0.4 mM up to $\sim 2 \times 10^{-5}$ cm s^{-1}. In the presence of 2 mM TP4 the TP3 permeabilites were significantly above ($\sim 4 \times 10^{-5}$ cm s^{-1}) the level of TP3 without TP4, and TP3 metabolism was totally inhibited. TP3 and TP4 showed a significant concentration dependent effect on the permeability of ^{3}H-mannitol. A hyperosmolarity effect of the peptide solutions was excluded. Transepithelial electrical resistance (TEER; $\sim 30\ \Omega$ cm^2) was unchanged by either TP3 or TP4. At 1 mM TP3 the mucosal-to-serosal permeability was four times higher than serosal-to-mucosal, indicating enzyme polarization. In reflection kinetics studies, TP3 degradation was slightly higher on the mucosal than on the serosal side. TP3 and TP4 followed the same nonlinear metabolism kinetics.

Conclusions. Increase in permeability at high TP concentrations involves competitive enzyme saturation combined with self-enhanced paracellular permeation.

KEY WORDS: nasal absorption; peptide absorption; nasal metabolism; aminopeptidases.

INTRODUCTION

Thymotrinan (TP3, Arg-Lys-Asp) is a biologically active fragment of the naturally occurring thymus hormone thymopoietin (1). The effects of thymic hormones focus on induction of T cell subpopulations and restoration of the impaired immune system (2). While TP3 and its homologue thymocartin (TP4, Arg-Lys-Asp-Val) are being investigated in clinical studies, thymopentin (TP5, Arg-Lys-Asp-Val-Tyr), i.e. thymopoietin 32–36, is registered for treatment of immunodeficiency diseases.

Delivery of therapeutic peptides across epithelia is limited by metabolic cleavage and low permeability. To overcome the enzymatic barrier, inhibitors have shown some potential (3). Permeation enhancers can cause morphological changes and membrane pertubations which are of great concern since such effects may enhance the permeation of environmental toxins (4). Therefore, competitive substrates may be preferred as toxicity problems related to chemical enhancers are avoided (3). To maximize competition, the inhibitory effect of di- and tripeptides can be improved by chemical modification; e.g. phosphinic acid dipeptide analogues inhibited nasal aminopeptidases (5). Furthermore, several peptides and proteins have shown to enhance their own paracellular transport, e.g. through phosphorylation of tight junctional components or Ca^{2+}-complexation. For Pz-peptide, Yen et al. (6) proposed tight junctional opening by mobilization of intracellular Ca^{2+}.

We demonstrated previously that at high concentrations TP4 permeability was augmented by one order of magnitude, presumably through local enzyme saturation. Therefore, the administration of small volumes of concentrated solutions was expected to enhance TP4 absorption (7). The objectives of this study were to compare concentration dependent permeabilities and metabolism kinetics of TP3 versus TP4. In particular, we investigate TP3 and TP4 as to their potential for substrate competition and effect on paracellular transport. For this purpose we present permeation and metabolism data in excised bovine nasal epithelium in combination with the permeability of a paracellular marker, ^{3}H-mannitol, and transepithelial electrical resistance (TEER).

MATERIALS AND METHODS

Materials

TP3 and TP4 were from Schwabe (Karlsruhe, Germany). Lys-Asp-Val, Asp-Val and Lys-Asp were from Bachem (Bubendorf, Switzerland), Arg from Sigma (Buchs, Switzerland). Ion composition of Krebs-Henseleit buffer (KHB) for permeation and metabolism studies was [mM] NaCl 117, KCl 4.7, $CaCl_2 \cdot 2\ H_2O$ 2.5, $MgSO_4 \cdot 7\ H_2O$ 1.2, $NaHCO_3$ 24.8, KH_2PO_4 1.2 and D-glucose 5.5 mM. Prior to use the freshly prepared buffer solution was oxygenated (95% O_2, 5% CO_2). All chemicals were of analytical grade (Fluka, Buchs, Switzerland). For chromatography, HPLC grade solvents were used. ^{3}H-mannitol (19.7 Ci mmol^{-1}) was from Du Pont de Nemours International (Le Grand-Saconnex, Switzerland).

Permeation Studies

Bovine nasal mucosa was obtained from freshly slaughtered cattle at the local slaughterhouse (Schlachthaus, Zurich, Switzerland) and excised as described by Lang et al. (7,8). For mucosal-to-serosal (m-to-s) and serosal-to-mucosal (s-to-m) permeation of TP3 and TP4 at 37°C, excised tissue samples were inserted between two diffusion half-cells (side-Bi-side™, Crownglass, Sommerville, NJ, USA).

Mucosal integrity was assessed using ^{3}H-mannitol in ethanol: water 9:1 (0.5 μCi mL^{-1} = 2.5×10^{-8} M). At 10, 45 and 60 min samples of 0.1 mL were taken from the receiver, added to 2 mL scintillation cocktail (Packard, Groningen, The

[1] Department of Applied BioSciences, Swiss Federal Institute of Technology Zurich (ETH), Irchel Campus, Winterthurerstrasse 190, CH-8057 Zurich, Switzerland.

[2] Genentech, Inc., 1 DNA Way, South San Francisco, California 94080-4990.

[3] Present address: Novo Nordisk Pharma AG, CH-8700 Küsnacht (ZH), Switzerland.

[4] To whom correspondence should be addressed. (e-mail: hmerkle@pharma.ethz.ch)

0724-8741/00/0200-0222$18.00/0

Netherlands) and counted (Beckmann Instruments, Fullerton, CA, USA).

Furthermore, we monitored the effect of 2 mM TP3 and TP4, respectively, on transepithelial electrical resistance (TEER) using an Ussing chamber set-up (Corning Costar, Acton, MA, USA) equipped with Ag-AgCl electrodes (Corning Costar). The VCC MC6 Multi-Channel Clamp (Physiologic Instruments, San Diego, CA, USA) was used to control the transepithelial current. Mixing was provided by a constant oxycarbon gas flow. After 30 min equilibration, KHB was replaced by fresh KHB. After another 30 min, 200 μL of a TP3 or TP4 solution was added on the mucosal side to reach a final concentration of 2 mM. Correspondingly, 200 μL KHB was added on the serosal side. TEERs were monitored during 90 min.

The osmolarities of a selection of TP3 and TP4 peptide solutions for the permeation studies were determined by freezing point depression using a Wescor osmometer 5500 (Baumann Medical, Wetzikon, Switzerland).

Calcium Complexation in Solution

Using a Ca^{2+}-selective membrane electrode we investigated whether TP peptides were capable of complexing extracellular Ca^{2+} responsible for the increase in tight junctional permeability. The membrane electrode based on the ionophore carrier ETH 1001 ([(−)-(R,R)-N,N′-Bis-[11-ethoxycarbonyl)-undecyl]-N,N′-4, 5-tetramethyl-3,6-dioxaoctane-diamide) was supplied by U. Spichiger, Center for Chemical Sensors/Biosensors and Bioanalytical Chemistry. Calibration was by Ca^{2+}-standard solutions (in KHB without Mg^{2+}). Every 2 min 1 mL peptide solution was added to 100 mL KHB (without Mg^{2+}), increasing the peptide concentration each time by 0.1 mM up to 1 mM. The potential measurements were performed at 25 ± 1°C. The 8-channel electrode monitor used was equipped with FET operational amplifiers AD515 KH (Analog Devices, Norwood, MA, USA), an active low pass filter in each channel for noise rejection and a latchable CMOS Multiplexer DG 529 (Siliconix GmbH, Filderstadt, Germany). A Solartron-Schumberger 7150 Digital Multimeter (resolution 1mV; Solartron Instrumentation Group, Farnborough, England) was used with remote control through an IEEE 488 interface.

Metabolism Studies

Metabolism of TP3 was studied using a reflection kinetics set-up as described by Lang et al. (7,9).

To compare metabolic activities at the mucosal versus the serosal side, nasal tissue was incubated with 1 mM TP3 solutions on both sides at the same time. Previously Lang et al. (7) demonstrated absence of relevant aminopeptidase leakage from excised mucosa.

HPLC of TP3 and TP4

For the analysis of TP3 and its metabolite Lys-Asp, a HPLC-method described by Heizmann et al. (10) was applied. For simultaneous analysis of TP3, TP4, and TP3 and TP4 metabolites, a gradient system was used. Solvent A was a mixture of 25% (v/v) acetonitrile and 75% (v/v) of 0.1% phosphoric acid containing 0.01 M 1-octanesulfonic acid sodium salt monohydrate and solvent B was a mixture of 35% (v/v) acetonitile and 65% (v/v) of 0.1% phosphoric acid containing 0.01 M 1-octanesulfonic acid sodium salt monohydrate. A linear gradient of 0 to 100% B in 7 min was used, followed by 100% B for 3 min.

Calculations

Effective permeability coefficients P_{eff} [cm s^{-1}] were calculated from linear segments of the concentration-time profiles in the receiver compartment. The pseudo steady-state metabolic turnover rates [μmol cm^{-2} s^{-1}] were calculated from the linear segments of the concentration-time profiles.

RESULTS

Permeation Studies

Figure 1 shows the P_{eff} values obtained as a function of initial TP3 donor concentration. At 0.1 and 0.2 mM no significant flux was measured. A major increase in permeability to $\sim 1.7 \cdot 10^{-5}$ cm s^{-1} was observed at ~0.4 mM TP3, indicating partial enzyme saturation. Higher TP3 concentration led to a moderate increase in P_{eff}, e.g. to $2.7 \cdot 10^{-5}$ at ~5 mM TP3. When TP3 permeation was studied in presence of 2 mM TP4, the mean TP3 permeability was significantly ($P = 0.001$) above the plateau (0.43 − 4.8 mM TP3) of the mean TP3 permeability without TP4, even at the lowest TP3 concentration studied, suggesting both inhibition of TP3 metabolism and enhancement of flux.

Lang et al. (7) studied the permeation of TP4 at 0.1, 0.4, and 0.9 mM initial concentration. The data are included in Fig. 1 (see insert), in combination with data from this work. Permeabilites at 0.1 and 0.4 mM TP4 were $\sim 0.2 \cdot 10^{-5}$ cm s^{-1} and $\sim 0.4 \cdot 10^{-5}$ cm s^{-1}, respectively. TP3 flux was below the detection limit. From 0.4 mM to 2.0 mM, P_{eff} of TP4 increased linearly, in contrast to the step profile determined for TP3. In the presence of a 10-fold excess of TP3 (2 mM),

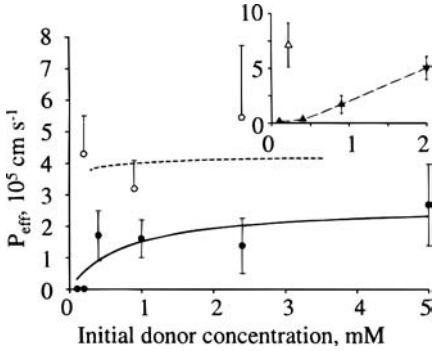

Fig. 1. Effective permeabilities P_{eff} [$10^5 \times$ cm s^{-1}] in bovine nasal mucosa as a function of the initial donor concentration [mM]. Permeabilities of TP3 alone (●), and in the presence of 2 mM TP4 (○). Insert: permeabilities of TP4 alone (▲; as adopted from (7)), and in the presence of 0.2 mM (▼) and 2 mM (△) TP3. Means ± SD, and means + SD, respectively; n = 3–4; SD partly within the points. The curves are empirical fits only to visualize the overall trend; solid line: TP3 alone, dashed line: TP3 in the presence of 0.2 mM TP4. Statistical significance (t-test, $P = 0.001$) of mean permeability of TP3 alone in plateau range (0.43–4.8 mM TP3, n = 13) versus mean permeability of TP3 (0.2–2.39 mM TP3; n = 10) in the presence of 2 mM TP4.

permeability of 0.2 mM TP4 was ten-fold higher ($\sim 7 \cdot 10^{-5}$ cm s^{-1}) as compared to permeability without TP3. In the gut this permeability level is typical for well-absorbed drugs.

To illustrate mucosal permeation and concurrent metabolism of TP3, at an initial concentration of, e.g., ~0.2 mM TP3 in the absence and the presence of 2 mM TP4, we simultaneously recorded peptide and metabolite concentrations in the donor and receiver compartments (Fig. 2a). In the absence of TP4 the permeation of intact TP3 through the mucosa into the receiver was minor and metabolite formation (Lys-Asp) was dominant (Fig. 2a, left panels). The main metabolic intermediate, Lys-Asp, is further cleaved, illustrated by its concentration peak at about 45 min on the receiver side. In contrast, the high TP3 concentration on the donor side caused enzyme saturation and inhibited degradation of Lys-Asp, causing a linear increase of Lys-Asp (Fig. 2a, upper left panel) in the donor.

In the presence of a 10-fold excess of TP4 (2 mM) in addition to ~0.2 mM initial TP3, we observed inhibition of TP3 metabolism. Thus, flux of intact TP3 into the receiver chamber was significantly increased (Fig. 2a, middle panels). On the donor side, TP3 degradation was reduced to one half as compared to the absence of TP4. The rate of formation of TP4 metabolites, Lys-Asp-Val and Asp-Val, is documented by an linear metabolite formation in both donor and receiver (Fig. 2a, right panels). In contrast to 2 mM TP4, 2 mM Lys-Asp failed to affect TP3 permeability. Corresponding to the absence of TP4, the permeability of TP3 was ~zero when Lys-Asp was present (data not shown). Thus, in contrast to TP4, Lys-Asp does not compete for the cleavage of TP3.

In addition to ~0.2 mM initial TP3 (Fig. 2a), permeation and metabolization were also monitored at ~1 mM initial TP3, both in the absence and presence of a two-fold excess of 2 mM TP4 (see Fig. 2b). When TP4 was absent, receiver concentrations of intact TP3 and its metabolite Lys-Asp were in a similar range (Fig. 2b, left panels). In the presence of 2 mM TP4 (Fig. 2b, middle panels), however, TP3 permeation into the receiver was only moderately improved. Initial metabolite concentration was lowered, but reached comparable levels after a lag time of ~30 min. Due to the higher initial TP3 concentrations, TP4 metabolites were reduced on both sides (Fig. 2a, right panels vs. Fig. 2b, right panels). Above all, the formation of Asp-Val was practically inhibited. All observations from Fig. 2a and 2b illustrate that TP3 and TP4 represent competitive substrates.

Large differences between m-to-s and s-to-m permeabilities of TP3 were found; at 1 mM TP3 the m-to-s permeability was about four times higher than the s-to-m permeability, i.e. $1.3 \pm 0.1 \cdot 10^{-5}$ cm s^{-1} versus $0.3 \pm 0.1 \cdot 10^{-5}$ cm s^{-1}, respectively, whereas the permeabilities of the paracellular marker ^{3}H-mannitol were equal in both directions in the presence of 1 mM TP3.

Figure 3 shows the concentration dependent effects of TP3 and TP4 on the permeability P_{eff} of ^{3}H-mannitol. In the presence of >1 mM TP3 and of ≥0.2 mM TP4, the P_{eff} of the paracellular marker increased, i.e. from $\sim 0.8 \cdot 10^{-4}$ cm s^{-1} to $\sim 1.5 \cdot 10^{-4}$ cm s^{-1}. The osmolarity of all TP peptide solutions used in this study was ~280 mmol kg^{-1}, excluding hyperosmolarity to explain the enhanced paracellular ^{3}H-mannitol flux. As calculated on the basis of a two-way ANOVA using an orthogonal segment of the data (see Fig. 3) the effects of both TP3 and TP4 on P_{eff} of the marker were significant ($P = 0.01$). The effects of TP3 and TP4 were not additive. In addition to the permeation of the integrity marker ^{3}H-mannitol, the TEER was also monitored. TEERs remained constant (~30 Ω cm^2) and did not change after the addition of 2 mM TP3 or 2 mM TP4. With leaky epithelia like nasal mucosa TEER is a poor predictor of paracellular permeability.

Calcium Complexation in Solution

Neither in presence of TP3 nor TP4 changes in the potential of the Ca^{2+}-solutions were measured by the Ca^{2+}-selective electrode. This indicated that the peptides cannot form complexes with Ca^{2+} in the buffer solution.

Metabolism Studies

The kinetics of the metabolic degradation of TP3 in nasal mucosa was first determined by reflection kinetics. In analogy to TP4 and TP5 (7), TP3 was metabolized through nasal enzymes by stepwise N-terminal cleavage of single amino acids. C-terminal cleavage of TP3 was insignificant, as no indication for the formation of Arg-Lys was detectable by HPLC (data not shown). Figure 4a–c represents concentration-time profiles of TP3 and its metabolite Lys-Asp for increasing initial TP3 concentrations. The percentage of metabolites decreased with increasing peptide concentration as saturation of the metabolic system was approached. At the lowest concentration (0.26 mM), the molar recovery rate after 90 min was ~78%, indicating further degradation of Lys-Asp to Lys and Asp, which were not detectable by the applied HPLC method. Because of saturation at higher TP3 concentrations, i.e. 1.0 mM and 1.5 mM, the molar recovery rates were higher and reached ~98%.

Derived from the linear cleavage profiles of TP3, the metabolic rate versus initial peptide concentration plot in Figure 4d depicts the (effective) non-linear metabolism kinetics of TP3. The figure also includes the corresponding TP4 kinetics derived from Lang et al. (7). The identity of the profiles suggests that both TPs were subject to the same cleavage mechanism and kinetics. This marks an intriguing contrast to the differences in the permeability versus TP concentration plots of TP3 and TP4 at low substrate concentrations, i.e. between 0 and 0.9 mM TP3 or TP4 (cf. Fig. 1).

As a second approach we compared the metabolic activities on the mucosal versus the serosal side; TP3 was degraded on both sides of the nasal mucosa, but mucosal metabolite concentrations were slightly higher than serosal ones, indicating moderate aminopeptidase activity polarization. Higher concentrations of Arg versus Lys-Asp suggest further cleavage of the dipeptide to single amino acids, which were undetectable by HPLC.

DISCUSSION

Here we demonstrate optimized nasal permeabilities, P_{eff}, of two thymopoietin (TP) derived oligopeptides, TP3 and TP4, in the high range of almost 10^{-4} cm s^{-1}. This result is attributed to (i) the saturation of mucosal aminopeptidase activity and (ii) the biochemical induction of self-enhancement. In the small intestine, permeabilities in this range are close to well-absorbed

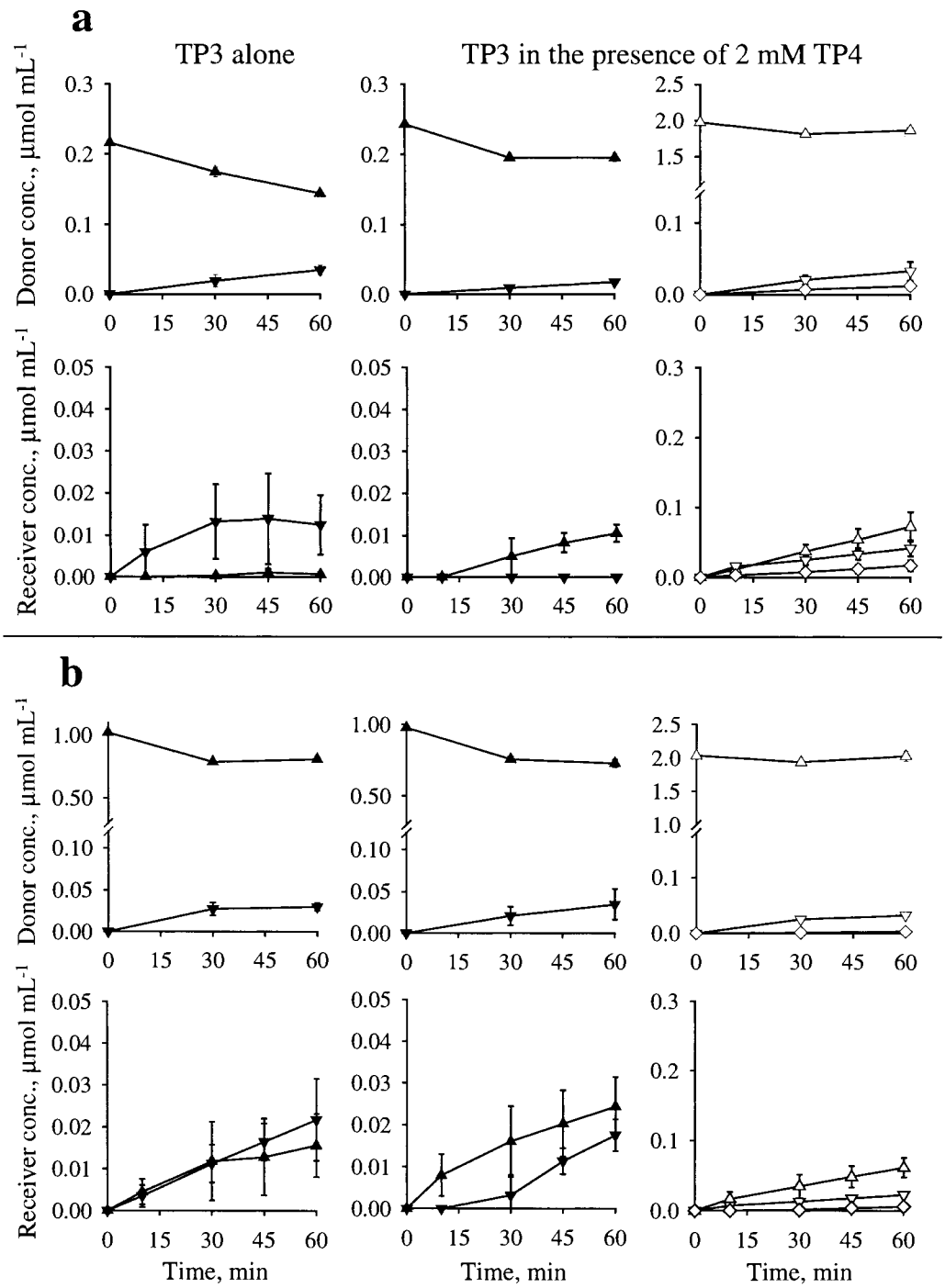

Fig. 2. Permeation and concurrent metabolic degradation of TP3 alone (left panel) in excised bovine nasal mucosa and the influence of the presence of 2 mM TP4 (middle and right panels). Initial TP3 donor concentrations were (a) 0.22 and 0.24 mM, respectively, and (b) 0.98 mM. Concentration-versus-time profiles of TP3 (▲) and of its metabolite Lys-Asp (▼), and of TP4 (△) and its metabolites Lys-Asp-Val (▽), and Asp-Val (◇). Means ± SD; n = 3–4; SD partly within the points.

lipophilic drugs. The low nasal bioavailabilities of many therapeutic peptides were previously shown to result from rapid enzymatic cleavage rather than low intrinsic permeabilities (12). In contrast, the permeabilities of metabolically stabilized peptides, e.g. octreotide and buserelin, were in the range of $\sim 2 - 4 \times \cdot 10^{-5}$ cm s^{-1} (13).

Metabolism

The saturable metabolic protection of TP3 by excess TP4 is assumed to result from competitive inhibition of the respective aminopeptidase(s). Similar effects were previously demonstrated in perfusion studies performed in intact nasal cavities

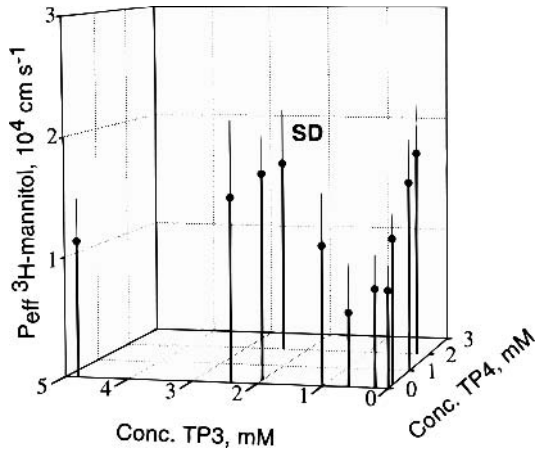

Fig. 3. Influence of the TP concentration on the permeability P_{eff} of the hydrophilic marker ^{3}H-mannitol as a parameter for tight junctional integrity. Permeabilities of ^{3}H-mannitol were measured in the presence of either TP3 or TP4, and both TP3 and TP4. Concentrations indicate initial concentrations of TP3 and TP4. Values are expressed as means +SD; n = 3–4. Two-way ANOVA of a selected orthogonal segment of data (TP3/TP4: 0.2/0, 2.4/0, 0.2/2.0, and 2.4/2.0; in mM; n = 4) indicated significant effects (P = 0.01) of both TP3 and TP4 on P_{eff}, but insignificant interaction of TP3 and TP4.

of anesthetized rats. The presence of Phe-Leu reduced efficiently the cleavage of leucine enkephalin (Tyr-Gly-Gly-Phe-Leu) to the des-tyrosine metabolite (14). The literature indicates that substrates with neutral, aromatic N-terminal amino acids reacted faster than those with neutral or basic aliphatic ones (15). In studies in intestinal brush-border membrane vesicles (BBMVs), dipeptides containing aromatic amino acids, e.g.

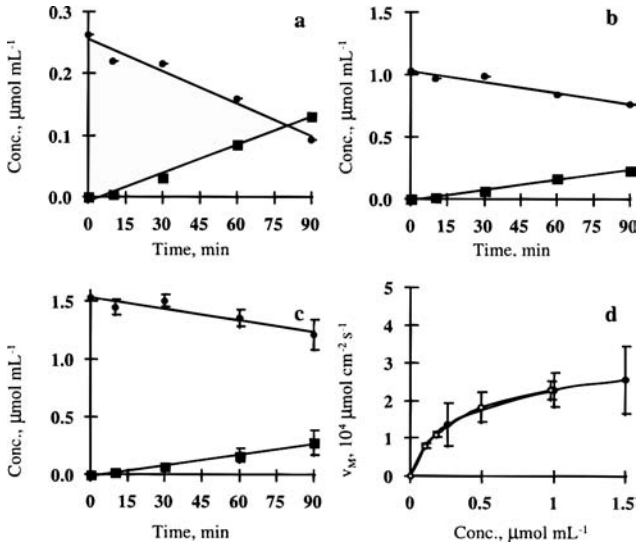

Fig. 4. Reflection kinetics studies of TP3 in bovine nasal mucosa. Concentration-versus-time profiles of TP3 (●) and its metabolite Lys-Asp (■) at different initial TP3 concentrations: (a) 0.3 mM, (b) 1.0 mM, and (c) 1.5 mM. The effect of the initial peptide concentration of TP3 (●) and TP4 (○) on saturable metabolism kinetics is shown in (d). TP4 values in (d) were adapted from (7). Means ± SD, n = 4; SD are partly within the points.

Ala-Phe and Ala-Tyr, better protected metkephamid (Tyr-D-Ala-Gly-Phe-N(Me)-Met-amide) from degradation than D-Ala-Gly, suggesting a hydrophobic binding pocket near the catalytic center of the enzyme (16).

Substrate Affinity to Nasal Aminopeptidase(s)

Incubation of TP peptides in the presence of intestinal brush-border membrane vesicles (BBMVs) and in pure aminopeptidase N solutions showed a trend for higher clearances and faster degradation rates for TP4 versus TP3 (10). Accordingly, differences in the permeability versus concentration plots of TP3 and TP4 at lower concentrations (Figure 1) are proposed to be caused by different affinities to the cleaving aminopeptidase(s). Particularly, the step profile in TP3 permeability at ~0.4 mM was in contrast to TP4 with its much lower P_{eff} at this concentration and a more sustained increase with concentration (Fig. 1, insert).

Furthermore, the degradation of 0.2 mM TP4 to Lys-Asp-Val was incompletely inhibited by 2 mM TP3, whereas the metabolic rate v_M of TP3 was zero in the reverse case of 0.2 mM TP3 in the presence of 2 mM TP4 (Fig. 2a). In the same context, a 10-fold excess of Lys-Asp was not capable to saturate the local aminopeptidases and protect TP3. Therefore, the affinity of this dipeptide to the binding domains of the involved enzyme(s) seems to be less specific and lower than those of TP3 and TP4.

Hypothetically, the hydrophobic C-terminal Val of TP4 may enhance its affinity to the hydrophobic pocket(s) of the enzyme(s). Currently, lens leucine aminopeptidase, an aminopeptidase N, is the only aminopeptidase with available 3D structure. Bestatin, a transition state analog of Phe-Leu, was shown to bind to two different hydrophobic pockets of lens leucine aminopeptidase (17). Taking this into account, the conformation of the smaller and less hydrophobic TP3 at the binding site is expected to be more flexible than TP4, thus reducing probability and formation of the initial enzyme-substrate complex. Indeed, increasing affinities for substrates with increasing peptide lengths were found for alanine aminopeptidase, a broad specificity aminopeptidase (18).

The proposed difference in aminopeptidase affinities of TP3 versus TP4 contrasts with the practically identical metabolism kinetics under reflection conditions (Figure 4d). Resulting from the steep substrate gradients typical for m-to-s permeation, saturation is restricted to the mucosal side. Under reflection kinetics concentrations are more evenly distributed. Hence, to detect differences in TP affinity, permeation kinetics is more sensitive than reflection kinetics.

Direction Specificity of Permeation

Because of its small size and high hydrophilicity, we expect TP3 to pass the nasal epithelium by passive diffusion via the paracellular route. The lack of large, lipophilic moieties restricts partitioning of this peptide from the aqueous environment into the cell membrane (19). When we assume evenly distributed aminopeptidase activity in the epithelium, no differences in the rates of permeation, m-to-s versus s-to-m, could be expected, except when (direction specific) active transport is involved. However, in epithelia with polarized enzyme distribution, direction specificity is no proof for active transport.

In the intestinal epithelium enzyme polarization is quite pronounced (20), as shown, e.g., by apical localization of dipeptidyl-peptidase IV in Caco-2/lymphocyte co-culture (21). The effect of polarized aminopeptidase distribution on direction specificity is illustrated by the direction specific transport of TP peptides through Caco-2 (22). Resulting from apical enzyme polarization, the apical-to-basolateral permeability was found ten-fold higher than in the reverse direction. Therefore, assuming polarized aminopeptidase distribution in the nasal mucosa, the 4-fold higher permeability m-to-s versus s-to-m, at 1 mM TP3 in the donor, indicates some degree of enzyme polarization on the mucosal side. This is consistent with the previous postulate of passive, paracellular permeation.

When incubating the tissue with TP3, simultaneously on the mucosal and the serosal side, only minor polarization became apparent (Fig. 5), mucosal metabolism being only 1.5-fold faster than serosal. This conflicts with the 4-fold difference between the m-to-s versus the s-to-m permeability shown before. We suggest that this conflict is explainable by the different experimental setups used. Whereas in the metabolism study both sides of the mucosa were simultaneously exposed to TP3, with comparable levels of enzyme saturation, only one side of the mucosa was saturated in the permeation study, i.e. either the mucosal or the serosal side. Assuming mucosal polarization, we expect mucosal saturation more efficient to enhance TP3 permeation than serosal saturation. In conclusion, we continue to propose that the 4-fold direction specificity of TP3 permeation results from mucosal enzyme polarization, i.e. not from active transport.

Self-Enhanced Permeability

Self-enhancement by TP peptides is concluded from the significant ~2-fold increase in ^{3}H-mannitol flux in the presence of TP3 and TP4 (Fig. 3). This is explained by a concentration-dependent self-enhancement of tight junctional permeability, making the tissue leakier. In presence of TP4, the permeability of TP3 was increased to a higher level than with TP3 alone (Fig. 1). The low TEER of this tissue, typical for leaky-type epithelia (13), explains why a decrease in TEER was not measurable. At low TEERs, ^{3}H-mannitol flux is more sensitive to monitor the paracellular pathway than TEER.

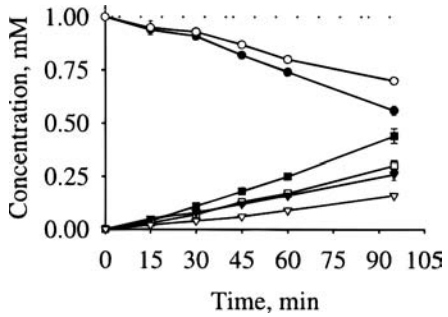

Fig. 5. Comparison of the metabolic degradation of 1 mM TP3 on the mucosal (full symbols) versus the serosal side (open symbols). Concentration-versus-time profiles of TP3 (● mucosal; ○ serosal), and of its metabolites Lys-Asp (▼ mucosal; ▽ serosal) and Arg (■ mucosal; □ serosal). Values are expressed as means ± SD, n = 2; SD partly within the points; dotted line represents total molar recovery (concentration of TP3 and Arg).

Previously, enhancement of the transport of paracellular markers was demonstrated for Pz-peptide (4-phenylazobenzyloxycarbonyl-Pro-Leu-Gly-Pro-D-Arg; (23)), leucine enkephalin (24), and polypeptide hormones, such as IGF I or II, tumor necrosis factor, and INF-γ (25). For Pz-peptide Yen et al. (6) proposed a G-protein coupled activation of phospholipase C. Other suggested mechanisms are the disruption of tight junctions by ATP depletion, protein kinase A inhibition and protein kinase C activation (25). For TP3 and TP4, control measurements using a Ca^{2+}-selective electrode ruled out Ca^{2+}-complexation. Therefore we exclude a direct effect on tight junctional integrity ("opening") by TP peptides.

Previously, the immunoregulatory action of another TP peptide, TP5, was related to its effect on T cells, mediated by an intracellular increase of cyclic GMP (26). In fact, we demonstrated different T cell types in bovine nasal epithelium (unpublished data). Hypothetically, upon interaction with mucosal T lymphocytes, TP peptides may increase cyclic GMP known to activate specific protein kinases that phosphorylate target proteins (27). Such protein kinase-mediated changes in tight junctional protein phosphorylation were reported to trigger junctional "opening" (25), a reasonable explanation for the observed modulation of ^{3}H-mannitol flux. This mechanism is still speculative. In conclusion, we propose that the increased permeability at high TP peptide concentrations involves competitive enzyme saturation combined with self-enhanced paracellular diffusion.

ACKNOWLEDGMENTS

We gratefully acknowledge the following contributions: Wei Zhang and Professor Ursula Spichiger (Center for Chemical Sensors/Biosensors and Bioanalytical Chemistry, ETH) for the Ca^{2+}-electrode measurements, and the local slaughterhouse (Schlachthaus AG Zürich) for bovine material.

REFERENCES

1. E. Rajnavolgyi, J. Kulics, M. Szilagyvari, L. Kisfaludy, O. Nyeki, I. Schon, and J. Gergely. The influence of new thymopoietin derivatives on the immune response of inbred mice. *Int. J. Immunopharmacol.* **8**:167–177 (1986).
2. L. Denes, B. Szende, G. Y. Hajos, L. Szporny, and K. Lapis. Therapeutic possibilities of thymopoietin fragments (TP3 and TP4) based on experimental animal models. *DECRDP* **13**:279–287 (1987).
3. A. Bernkop-Schnürch. The use of inhibitory agents to overcome the enzymatic barrier to perorally administered therapeutic peptides and proteins. *J. Contr. Rel.* **52**:1–16 (1998).
4. L. L. Wearley. Recent progress in protein and peptide delivery by noninvasive routes. *Crit. Rev. Ther. Drug Carrier Syst.* **8**:331–394 (1991).
5. M. A. Hussain, M. S. L. Lim, K. S. Raghavan, N. J. Rogers, R. Hidalgo, and C. A. Kettner. A phosphinic acid dipeptide analogue to stabilize peptide drugs during their intranasal absorption. *Pharm. Res.* **9**:626–628 (1992).
6. W. C. Yen, Y. Higashi, and V. H. L. Lee. Intestinal paracellular peptide transport: Mobilization of intracellular calcium as a mechanism of tight junctional opening by 4-phenylazo-benzoxycarbonyl-Pro-Leu-Gly-Pro-D-Arg (Pz-peptide) in the rabbit descending colon and Caco-2 cell monolayers. *J. Contr. Rel.* **46**:5–15 (1997).
7. S. Lang, R. Oschmann, B. Traving, P. Langguth, and H. P. Merkle. Transport and metabolic pathway of thymocartin (TP4) in excised bovine nasal mucosa. *J. Pharm. Pharmacol.* **48**:1190–1196 (1996).
8. S. Lang, B. Rothen-Rutishauser, J.-C. Perriard, M. C. Schmidt, and H. P. Merkle. Permeation and pathways of human calcitonin

(hCT) across excised bovine nasal mucosa. *Peptides* **19**:599–607 (1998).
9. S. R. Lang, W. Staudenmann, P. James, H.-J. Manz, R. Kessler, B. Galli, H.-P. Moser, A. Rummelt, and H. P. Merkle. Proteolysis of human calcitonin in excised bovine nasal mucosa: elucidation of the metabolic pathway by liquid secondary ionization mass spectrometry (LSIMS) and matrix assisted laser desorption ionization mass spectometry (MALDI). *Pharm. Res.* **13**:1679–1685 (1996).
10. J. Heizmann, P. Langguth, A. Biber, R. Oschmann, H. P. Merkle, and S. Wolffram. Enzymatic cleavage of thymopoietin oligopeptides by pancreatic and intestinal brush-border enzymes. *Peptides* **17**:1083–1089 (1996).
11. I. K. Chun, M. L. Lee, and Y. W. Chien. Methionine enkephalin. I. Kinetics of degradation in buffered solutions and metabolism in various mucosae extracts. *Pharm. Res.* **7**:S–48 (1990).
12. A. A. Hussain, K. Iseki, M. Kagoshima, and L. W. Dittert. Hydrolysis of peptides in the nasal cavity of humans. *J. Pharm. Sci.* **79**:947–948 (1990).
13. M. C. Schmidt, H. Peter, S. R. Lang, G. Ditzinger, and H. P. Merkle. In vitro cell models to study nasal mucosal permeability and metabolism. *Adv. Drug Del. Rev.* **29**:51–79 (1998).
14. A. Hussain, J. Faraj, Y. Aramaki, and J. E. Truelove. Hydrolysis of leucine enkephalin in the nasal cavity of the rat—A possible factor in the low bioavailability of nasally administered peptides. *Biochem. Biophys. Res. Commun.* **133**:923–928 (1985).
15. M. A. Hussain, R. Seetharam, R. R. Wilk, B. J. Aungst, and C. A. Kettner. Nasal mucosal metabolism and absorption of pentapeptide enkephalin analogs having varying N-terminal amino acids. *J. Pharm. Sci.* **84**:62–64 (1995).
16. P. Langguth, V. Bohner, J. Heizmann, H. P. Merkle, S. Wolffram, G. L. Amidon, and S. Yamashita. The challenge of proteolysis enzymes in intestinal peptide delivery. *J. Contr. Rel.* **46**:39–57 (1997).
17. A. Taylor. Aminopeptidases: Structure and function. *FASEB J.* **7**:290–298 (1993).
18. M. Smyth and G. O'Cuinn. Dipeptidyl aminopeptidase III of guinea-pig brain: specificity for short oligopeptide sequences. *J. Neurochem.* **63**:1439–1445 (1994).
19. P. S. Burton, R. A. Conradi, and A. R. Hilgers. Transcellular mechanism of peptide and protein absorption: passive aspects. *Adv. Drug Deliv. Rev.* **7**:365–386 (1991).
20. R. H. Erickson. In M. D. Taylor, G. L. Amidon (eds.), *Peptide-based drug design*, ACS Washington, DC, 1995; pp 23–46.
21. S. Kerneis, A. Bogdanova, J. P. Kraehenbuhl, and E. Pringault. Conversion by Peyer's patch lymphocytes of human enterocytes into M cells that transport bacteria. *Science* **277**:949–952 (1997).
22. J. Heizmann, H. P. Merkle, and P. Langguth. Permeation of thymopoietin oligopeptides through Caco-2 cell monolayers. *Proceed. Int. Symp. Control. Rel. Bioact. Mater.* 681–682 (1998).
23. W. C. Yen and V. H. L. Lee. Penetration enhancement effect of Pz-peptide, a paracellularly transported peptide, in rabbit intestinal segments and Caco-2 cell monolayers. *J. Contr. Rel.* **36**:25–37 (1995).
24. S. E. Thompson, J. Cavitt, and K. L. Audus. Leucine enkephalin effects on paracellular and transcellular permeation pathways across brain microvessel endothelial cell monolayers. *J. Cardiovasc. Pharmacol.* **24**:818–825 (1994).
25. J. Hochman and P. Artursson. Mechanisms of absorption enhancement and tight junction regulation. *J. Contr. Rel.* **29**:253–267 (1994).
26. G. A. Heavner, T. Audhya, D. Kroon, and G. Goldstein. Structural requirements for the biological activity of thymopentin analogs. *Arch. Biochem. Biophys.* **242**:248–255 (1985).
27. B. Alberts, D. Bray, J. Lewis, M. Raff, K. Roberts, and J. D. Watson *Molecular biology of the cell, 2nd edition*; Garland Publishing Inc.: New York, 1989.